

## BES RESULTS ON CHARMONIUM DECAYS AND TRANSITIONS

FREDERICK A. HARRIS  
(FOR THE BES COLLABORATION)

*Department of Physics and Astronomy, The University of Hawaii,  
Honolulu, Hawaii 96822, USA  
E-mail: fah@phys.hawaii.edu*

Results are reported based on samples of 58 million  $J/\psi$  and 14 million  $\psi(2S)$  decays obtained by the BESII experiment. Improved branching fraction measurements are determined, including branching fractions for  $J/\psi \rightarrow \pi^+\pi^-\pi^0$ ,  $\psi(2S) \rightarrow \pi^0 J/\psi$ ,  $\eta J/\psi$ ,  $\pi^0\pi^0 J/\psi$ , anything  $J/\psi$ , and  $\psi(2S) \rightarrow \gamma\chi_{c1}, \gamma\chi_{c2} \rightarrow \gamma\gamma J/\psi$ . Using 14 million  $\psi(2S)$  events,  $f_0(980)f_0(980)$  production in  $\chi_{c0}$  decays and  $K^*(892)^0\bar{K}^*(892)^0$  production in  $\chi_{cJ}$  ( $J = 0, 1, 2$ ) decays are observed for the first time, and branching ratios are determined.

## 1 Introduction

The Beijing Spectrometer (BES) <sup>1,2</sup> is a general purpose solenoidal detector at the Beijing Electron Positron Collider (BEPC). BEPC operates in the center of mass energy range from 2 to 5 GeV with a luminosity at the  $J/\psi$  energy of approximately  $5 \times 10^{30} \text{ cm}^{-2}\text{s}^{-1}$ . More details on the analyses described here can be found in the references.

## 2 $\psi(2S) \rightarrow \gamma\gamma J/\psi$ and $XJ/\psi$

Experimental results for the processes  $\psi(2S) \rightarrow \pi^0 J/\psi$ ,  $\eta J/\psi$ , and  $\gamma\chi_{c1,2}$  are few and date mainly from the 1970s and 80s. <sup>3</sup> In an analysis based on a sample of  $14.0 \times 10^6$   $\psi(2S)$  events collected with the BESII detector, events of the type  $\psi(2S) \rightarrow \gamma\gamma J/\psi$ ,  $J/\psi \rightarrow e^+e^-$  and  $\mu^+\mu^-$  are used to measure branching ratios for  $\psi(2S) \rightarrow \pi^0 J/\psi$ ,  $\eta J/\psi$ , and  $\gamma\chi_{c1,2}$ . <sup>4</sup> Fig. 1 shows, after a cut to remove the background under the  $\psi(2S) \rightarrow \pi^0 J/\psi$  signal from  $\psi(2S) \rightarrow \gamma\chi_{c1,2}$ , the distribution of  $\gamma\gamma$  invariant mass,  $M_{\gamma\gamma}$ . The branching fractions obtained for this and the other channels are listed in Table 1. The BES  $B(\psi(2S) \rightarrow \pi^0 J/\psi)$  measurement has improved precision by more than a factor of two compared with other experiments, and the  $\psi(2S) \rightarrow \eta J/\psi$  branching fraction is the most accurate single measurement.

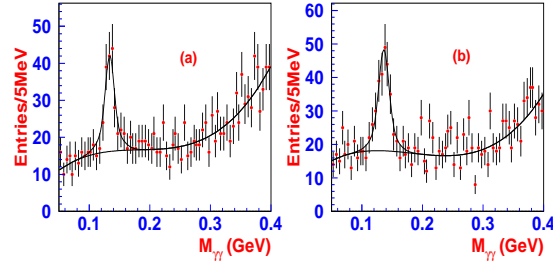


Figure 1. Two photon invariant mass distribution for candidate  $\psi(2S) \rightarrow \pi^0 J/\psi$  events for (a)  $\gamma\gamma e^+e^-$  and (b)  $\gamma\gamma\mu^+\mu^-$ .

In another analysis, based on approximately  $4 \times 10^6$   $\psi(2S)$  events obtained with the BESII detector, <sup>1</sup> a different technique is used for measuring branching fractions for the inclusive decay  $\psi(2S) \rightarrow \text{anything} J/\psi$ , and the exclusive processes. <sup>5</sup> Inclusive  $\mu^+\mu^-$  pairs are reconstructed, and the inclusive branching fraction is determined from the number of events in the  $J/\psi \rightarrow \mu^+\mu^-$  peak in the  $\mu^+\mu^-$  invariant mass distribution. The exclusive branching fractions are determined from fits to the distribution of masses recoiling from the  $J/\psi$ ,  $m_X$ , with Monte-Carlo determined distributions for each individual channel, where  $m_X$  is determined from energy and momentum conservation.

To separate  $\psi(2S) \rightarrow J/\psi\pi^0\pi^0$  and  $\psi(2S) \rightarrow J/\psi\pi^+\pi^-$  events,  $m_X$  histograms

Table 1. Results from  $\psi(2S) \rightarrow \gamma\gamma J/\psi$ 

Channel	$\pi^0 J/\psi$		$\eta J/\psi$	
Final state	$\gamma\gamma e^+e^-$	$\gamma\gamma\mu^+\mu^-$	$\gamma\gamma e^+e^-$	$\gamma\gamma\mu^+\mu^-$
B (%)	$0.139 \pm 0.020 \pm 0.012$	$0.147 \pm 0.019 \pm 0.013$	$2.91 \pm 0.12 \pm 0.21$	$3.06 \pm 0.14 \pm 0.25$
Combined (%)	$0.143 \pm 0.014 \pm 0.012$		$2.98 \pm 0.09 \pm 0.23$	
PDG (%) <sup>3</sup>	$0.096 \pm 0.021$		$3.16 \pm 0.22$	
Channel	$\gamma\chi_{c1}$		$\gamma\chi_{c2}$	
Final state	$\gamma\gamma e^+e^-$	$\gamma\gamma\mu^+\mu^-$	$\gamma\gamma e^+e^-$	$\gamma\gamma\mu^+\mu^-$
B (%)	$8.73 \pm 0.21 \pm 1.00$	$9.11 \pm 0.24 \pm 1.12$	$7.90 \pm 0.26 \pm 0.88$	$8.12 \pm 0.23 \pm 0.99$
Combined (%)	$8.90 \pm 0.16 \pm 1.05$		$8.02 \pm 0.17 \pm 0.94$	
PDG (%) <sup>3</sup>	$8.4 \pm 0.8$		$6.4 \pm 0.6$	

for events with (see Fig. 2) and without additional charged tracks are fit simultaneously. Ratios of the studied branching fractions to that for  $B(\psi(2S) \rightarrow \pi^+\pi^- J/\psi)$  are reported. This has that advantage that many of the systematic errors largely cancel.

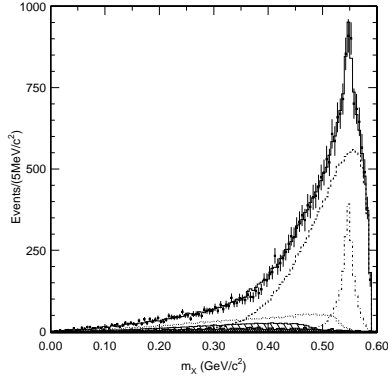


Figure 2. Fit of the  $m_X$  distribution for  $\psi(2S) \rightarrow XJ/\psi, J/\psi \rightarrow \mu^+\mu^-$  events with no additional charged tracks. Shown are the data (points with error bars), the component histograms, and the final fit. For the components, the large, long-dash histogram is  $\psi(2S) \rightarrow J/\psi\pi\pi$ , the narrow, dash-dot histogram is  $\psi(2S) \rightarrow J/\psi\eta$ , the broad, short-dashed histogram is  $\psi(2S) \rightarrow \gamma\chi_{c1}, \chi_{c1} \rightarrow \gamma J/\psi$ , the broad, hatched histogram is  $\psi(2S) \rightarrow \gamma\chi_{c2}, \chi_{c2} \rightarrow \gamma J/\psi$ , and the lowest cross-hatched histogram is the combined  $e^+e^- \rightarrow \gamma\mu^+\mu^-$  and  $e^+e^- \rightarrow \psi(2S), \psi(2S) \rightarrow (\gamma)\mu^+\mu^-$  background. The final fit is the solid histogram.

The final branching fraction ratios and branching fractions are shown in Table 2.  $B(J/\psi \text{ anything})/B(\pi^+\pi^- J/\psi)$  and  $B(\eta J/\psi)/B(\pi^+\pi^- J/\psi)$  have smaller errors

than the previous results. The agreement with the PDG fit results is good, and  $B(\eta J/\psi)$  agrees well with that from  $\psi(2S) \rightarrow \gamma\gamma J/\psi$  decays above.

### 3 $\chi_{cJ}$ decays

Using  $\psi(2S) \rightarrow \gamma\chi_{cJ}$  radiative decays in the 14 million  $\psi(2S)$  event sample, BES recently studied  $\chi_{cJ} \rightarrow p\bar{p}$ <sup>6</sup> and  $\Lambda\bar{\Lambda}$ .<sup>7</sup> Here, we report on the analysis of  $\pi^+\pi^-\pi^+\pi^-$  final states from  $\chi_{c0}$  decays, where evidence for  $f_0(980)f_0(980)$  production is obtained for the first time,<sup>8</sup> and on the analysis of  $\pi^+\pi^-K^+K^-$  final states from  $\chi_{cJ}$  ( $J = 0, 1, 2$ ) decays, where signals of  $\chi_{cJ}$  decays to  $K^*(892)^0\bar{K}^*(892)^0$  are observed for the first time.<sup>9</sup>

The  $\pi^+\pi^-\pi^+\pi^-$  invariant mass distribution for  $\psi(2S) \rightarrow \gamma\pi^+\pi^-\pi^+\pi^-$  events that satisfy a four-constraint kinematic fit is shown in Fig. 3. There are clear peaks corresponding to the  $\chi_{cJ}$  states. Figure 4 shows the scatter plot of  $\pi^+\pi^-$  versus  $\pi^+\pi^-$  invariant mass for events in the  $\chi_{c0}$  peak. A clear  $f_0(980)f_0(980)$  signal can be seen. There are hints of  $\rho^0\rho^0$  and  $f_0(1370)f_0(1370)$  (or  $f_2(1270)f_2(1270)$ ) signals.

The number of  $f_0(980)f_0(980)$  events and the corresponding background are estimated from the scatter plot. The resulting branching fraction is  $\mathcal{B}(\psi(2S) \rightarrow \gamma\chi_{c0} \rightarrow \gamma f_0(980)f_0(980) \rightarrow \gamma\pi^+\pi^-\pi^+\pi^-) = (6.5 \pm 1.6 \pm 1.3) \times 10^{-5}$ , and using the PDG2004 value for  $\mathcal{B}(\psi(2S) \rightarrow \gamma\chi_{c0})$ <sup>3</sup>, we obtain

Table 2. Branching ratios and branching fractions from  $\psi(2S) \rightarrow XJ/\psi$ . PDG04-exp results are single measurements or averages of measurements, while PDG04-fit are results of their global fit to many experimental measurements. The BES results in the second half of the table are calculated using the PDG04 value of  $B_{\pi\pi} = B(\psi(2S) \rightarrow J/\psi\pi^+\pi^-) = (31.7 \pm 1.1)\%$ .

Case	This result	PDG04-exp	PDG04-fit
$B(J/\psi \text{ (anything)})/B_{\pi\pi}$	$1.867 \pm 0.026 \pm 0.055$	$2.016 \pm 0.150$	$1.821 \pm 0.036$
$B(J/\psi\pi^0\pi^0)/B_{\pi\pi}$	$0.570 \pm 0.009 \pm 0.026$	-	$0.59 \pm 0.05$
$B(J/\psi\eta)/B_{\pi\pi}$	$0.098 \pm 0.005 \pm 0.010$	$0.091 \pm 0.021$	$0.100 \pm 0.008$
$B(\gamma\chi_{c1})B(\chi_{c1} \rightarrow \gamma J/\psi)/B_{\pi\pi}$	$0.126 \pm 0.003 \pm 0.038$	$0.085 \pm 0.021$	$0.084 \pm 0.006$
$B(\gamma\chi_{c2})B(\chi_{c2} \rightarrow \gamma J/\psi)/B_{\pi\pi}$	$0.060 \pm 0.000 \pm 0.028$	$0.039 \pm 0.012$	$0.041 \pm 0.003$
$B(J/\psi \text{ (anything)}) (\%)$	$59.2 \pm 0.8 \pm 2.7$	$55 \pm 7$	$57.6 \pm 2.0$
$B(J/\psi\pi^0\pi^0) (\%)$	$18.1 \pm 0.3 \pm 1.0$	-	$18.8 \pm 1.2$
$B(J/\psi\eta) (\%)$	$3.11 \pm 0.17 \pm 0.31$	$2.9 \pm 0.5$	$3.16 \pm 0.22$
$B(\gamma\chi_{c1})B(\chi_{c1} \rightarrow \gamma J/\psi) (\%)$	$4.0 \pm 0.1 \pm 1.2$	$2.66 \pm 0.16$	$2.67 \pm 0.15$
$B(\gamma\chi_{c2})B(\chi_{c2} \rightarrow \gamma J/\psi) (\%)$	$1.91 \pm 0.01 \pm 0.86$	$1.20 \pm 0.13$	$1.30 \pm 0.08$

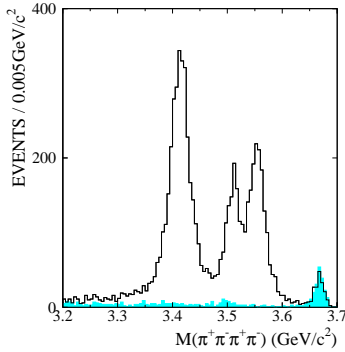


Figure 3. The  $\pi^+\pi^-\pi^+\pi^-$  invariant mass spectrum for selected  $\psi(2S) \rightarrow \gamma\pi^+\pi^-\pi^+\pi^-$  events. The shadow histogram shows the spectrum for Monte Carlo simulated background events. The highest mass peak corresponds to charged track final states that are kinematically fit with an unassociated photon.

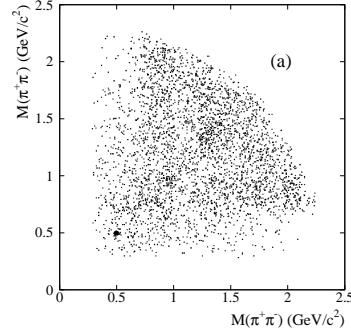


Figure 4. Scatter plot of  $\pi^+\pi^-$  versus  $\pi^+\pi^-$  invariant mass for selected  $\gamma\pi^+\pi^-\pi^+\pi^-$  events with  $\pi^+\pi^-\pi^+\pi^-$  mass in the  $\chi_{c0}$  peak.

$\mathcal{B}(\chi_{c0} \rightarrow f_0(980)f_0(980) \rightarrow \pi^+\pi^-\pi^+\pi^-) = (7.6 \pm 1.9 \text{ (stat)} \pm 1.6 \text{ (syst)}) \times 10^{-4}$ . This may help in understanding the nature of the controversial  $f_0(980)$ .

A similar analysis has been done for  $\psi(2S) \rightarrow \gamma\pi^+\pi^-K^+K^-$ . The invariant mass distribution for the  $\pi^+\pi^-K^+K^-$  events that satisfy the 4C kinematic fit shows clear peaks corresponding to the  $\chi_{cJ}$  states. The scatter plots of  $K^-\pi^+$  versus  $K^+\pi^-$  invariant masses for events in each of the  $\chi_{cJ}$  peaks show clear  $K^*(892)^0\bar{K}^*(892)^0$  signals in all  $\chi_{cJ}$  decays. After sideband subtraction, the  $K^*(892)^0\bar{K}^*(892)^0$  mass spectrum is fitted with three Breit-Wigner functions folded with Gaussian resolutions, as shown in Fig. 5.

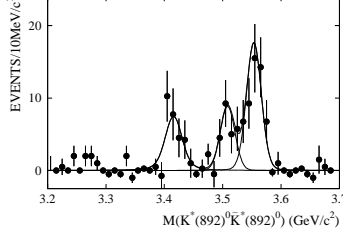


Figure 5. The  $K^*(892)^0 \bar{K}^*(892)^0$  invariant mass spectrum for  $\psi(2S) \rightarrow \gamma K^*(892)^0 \bar{K}^*(892)^0$  events fitted with three resolution smeared Breit-Wigner functions.

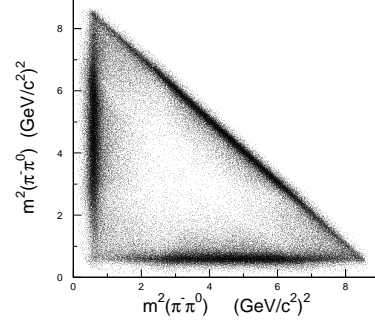


Figure 6. The Dalitz plot for  $J/\psi \rightarrow \pi^+\pi^-\pi^0$ .

The preliminary branching fractions are  $\mathcal{B}(\psi(2S) \rightarrow \gamma\chi_{c0} \rightarrow \gamma K^*(892)^0 \bar{K}^*(892)^0) = (1.53 \pm 0.29 \pm 0.26) \times 10^{-4}$ ,  $\mathcal{B}(\psi(2S) \rightarrow \gamma\chi_{c1} \rightarrow \gamma K^*(892)^0 \bar{K}^*(892)^0) = (1.40 \pm 0.27 \pm 0.22) \times 10^{-4}$ ,  $\mathcal{B}(\psi(2S) \rightarrow \gamma\chi_{c2} \rightarrow \gamma K^*(892)^0 \bar{K}^*(892)^0) = (3.11 \pm 0.36 \pm 0.48) \times 10^{-4}$ , and with the PDG world average values of  $\psi(2S) \rightarrow \gamma\chi_{cJ}$ <sup>3</sup>, we get  $\mathcal{B}(\chi_{c0} \rightarrow K^*(892)^0 \bar{K}^*(892)^0) = (1.78 \pm 0.34 \pm 0.34) \times 10^{-3}$ ,  $\mathcal{B}(\chi_{c1} \rightarrow K^*(892)^0 \bar{K}^*(892)^0) = (1.67 \pm 0.32 \pm 0.31) \times 10^{-3}$ ,  $\mathcal{B}(\chi_{c2} \rightarrow K^*(892)^0 \bar{K}^*(892)^0) = (4.86 \pm 0.56 \pm 0.88) \times 10^{-3}$ .

#### 4 $B(J/\psi \rightarrow \pi^+\pi^-\pi^0)$

The largest  $J/\psi$  decay involving hadronic resonances is  $J/\psi \rightarrow \rho(770)\pi$ . Its branching fraction has been reported by many experimental groups<sup>3</sup> assuming all  $\pi^+\pi^-\pi^0$  final states come from  $\rho(770)\pi$ . Here, we present two independent measurements of this branching fraction.<sup>10</sup>

The first, using 58 million  $J/\psi$  events, is an absolute measurement of  $J/\psi \rightarrow \pi^+\pi^-\pi^0$  directly, where 219691  $\pi^+\pi^-\pi^0$  candidates are selected. The branching fraction is  $B(J/\psi \rightarrow \pi^+\pi^-\pi^0) = (21.84 \pm 0.05 \pm 2.01) \times 10^{-3}$ . The Dalitz plot of  $m_{\pi^+\pi^0}$  versus  $m_{\pi^-\pi^0}$  is shown in Fig. 6. Three bands are clearly visible in the plot, corresponding to  $J/\psi \rightarrow \rho\pi$ ;  $J/\psi \rightarrow \pi^+\pi^-\pi^0$  is strongly dominated by  $\rho\pi$ .

The second measurement, based on 14 million  $\psi(2S)$  events, is a relative measurement obtained from a comparison of the rates for

$$\begin{aligned} \psi(2S) \rightarrow \pi^+\pi^- J/\psi & \\ \hookrightarrow \pi^+\pi^-\pi^0 & \quad (I) \\ \text{and } \hookrightarrow \mu^+\mu^- & \quad (II) \end{aligned}$$

Here, many systematic errors mostly cancel.

The branching fraction obtained is  $B(J/\psi \rightarrow \pi^+\pi^-\pi^0) = (20.91 \pm 0.21 \pm 1.16) \times 10^{-3}$ . The results of the two measurements are in good agreement. Their weighted mean is

$$B(J/\psi \rightarrow \pi^+\pi^-\pi^0) = (2.10 \pm 0.12)\%.$$

The result obtained is higher than those of previous measurements and has better precision.

## 5 Acknowledgments

I want to thank my BES colleagues for their efforts on the work reported here.

## References

1. J. Z. Bai *et al.*, (BES Collab.), *Nuc. Inst. Meth.* **A344**, 319 (1994).
2. J. Z. Bai *et al.*, (BES Collab.), *Nuc. Inst. Meth.* **A458**, 627 (2001).
3. S. Eidelman *et al.*, (Particle Data Group), *Phys. Lett.* **B592**, 1 (2004).

4. M. Ablikim *et al.*, (BES Collab.), *Phys. Rev.* **D70**, 012006 (2004).
5. M. Ablikim *et al.*, BES Collab., *Phys. Rev.* **D70**, 012003 (2004).
6. J. Z. Bai *et al.*, BES Collab., *Phys. Lett.* **B591**, 42 (2004).
7. J. Z. Bai *et al.*, BES Collab., *Phys. Rev.* **D67**, 112001 (2004).
8. M. Ablikim *et al.*, BES Collab., accepted by *Phys. Rev.* **D**, hep-ex/0406079.
9. M. Ablikim *et al.*, BES Collab., submitted to *Phys. Rev.* **D**, hep-ex/0408012.
10. J. Z. Bai *et al.*, (BES Collab.), *Phys. Rev.* **D70**, 012005 (2004).